Journal of Hazardous Materials 180 (2010) 98–105

Contents lists available at ScienceDirect

Journal of Hazardous Materials

journal homepage: www.elsevier.com/locate/jhazmat

Preparation and adsorption performance of a novel bipolar PS-EDTA resin in aqueous phase

Liuqing Yang[a], Yanfeng Li[a,*], Liyuan Wang[a], Yun Zhang[a], Xiaojie Ma[a], Zhengfang Ye[b]

[a] State Key Laboratory of Applied Organic Chemistry, College of Chemistry and Chemical Engineering, College of Resources and Environment, Institute of Biochemical Engineering & Environmental Technology, Lanzhou University, Lanzhou 730000, PR China
[b] Department of Environmental Engineering, Institute of Environmental Sciences & Technology, Peking University, Beijing 100871, PR China

ARTICLE INFO

Article history:
Received 8 January 2010
Received in revised form 7 March 2010
Accepted 26 March 2010
Available online 3 April 2010

Keywords:
Chelating resin
Synthesis
Silver adsorption
Heavy metal removal

ABSTRACT

A novel chelating resin containing many amino and carboxyl functional groups, PS-EDTA resin, was prepared from chloromethylated polystyrene bead by reacting with ethylenediamine and chloroacetate in aqueous phase in sequence. The structure of PS-EDTA resin was characterized by means of infrared spectroscopy, scanning electron microscopy, surface area analysis and thermogravimetry. Adsorption behavior of the resin for Ag (I) ions in aqueous solutions was investigated by batch experiments. The results indicated that the adsorption removal of PS-EDTA resin for Ag (I) could achieve more than 99.9% at pH values of 5.0 with an initial Ag (I) concentration of 60.0 mg/L within 2 h. The maximum removal capacity of PS-EDTA toward Ag (I) was found to be almost 3314.97 mg/g at 25 °C. In addition, adsorption kinetic data were described by pseudo-second-order equation and the equilibrium data fitted very well with the Freundlich model. It was found that the PS-EDTA resin had excellent adsorption properties for Ag (I), so it should be a promising composite adsorbent with application in the recovery of Ag (I) ions from aqueous environment.

1. Introduction

The pollution of toxic heavy-metal ions from many industries, such as metal plating, mining, painting, smelting, car radiator manufacturing, petroleum refining and agricultural activities, has already become a worldwide problem that endangers the environment and health of human beings [1]. Consequently, the health risks due to the accumulation of heavy metals in the human body are becoming a matter of growing concern, this has led to regulatory actions to reduce the exposure of humans to heavy metal on many fronts, and removal of toxic heavy metal ions has received great attention in recent years [2,3]. That toxic heavy metal ions were discharged into the environment will be serious pollution problems affecting water quality especially. Several methods have been applied during many years for the elimination of heavy metal ions present in the industrial wastewaters [4–11]. The traditional methods commonly used for removal of heavy metal ions from aqueous solution include ion-exchange [5], solvent extraction, chemical precipitation [6], nano-filtration [7], reverse osmosis [8] and adsorption [9–11]. Among all of these treatment processes, the adsorption using suitable adsorbents should be considered one of the most effective and economical methods in terms of and the simplicity of design and easiness of operation [1,12,13], which even can be used to applications in the purification of drinking water. Great efforts have been contributed to the development of new adsorbents like activated carbon, chelating resin, hydroxyapatite, silica gel, zeolite, clay, goethite, modified mineral adsorbent, and other functional polymers each has its merits and limitations in practice [14–17]. Nonetheless, the cost and regeneration of adsorbents are the key factors influencing their application in practice, especially for the treatment of large volume of wastewater. To keep up with this step, many researchers have deeply tried to find out low-cost, efficient, and reusable adsorbents antidotes for the adsorptive removal of heavy metal [18,19].

During the past decade, several metal-retaining resin, containing a variety of complexion or chelating ligands, have been reported to efficiently remove heavy metals [20–23]. Synthetic polymers containing amino, thio, oxo, carboxyl, phosphoryl, and so on have been developed. In particular, the amino/carboxyl group on an adsorbent has been found to be one of the most effective chelate functional groups for adsorption or removal of heavy metal ions from an aqueous solution [24–30]. It has also been reported that the amine groups can provide reactive sites for specific adsorption of various metal ions [30–34]. In the late 1980s and early 1990s, EDTA (ethylene diamine tetraacetic acid) was suggested as a nice small molecular chelating agent for exhibiting extremely high metal-chelating capacity because it con-

* Corresponding author.
E-mail address: liyf@lzu.edu.cn (Y. Li).

0304-3894/$ – see front matter © 2010 Elsevier B.V. All rights reserved.
doi:10.1016/j.jhazmat.2010.03.111

tains abundant functions being able to chelate with metal ions [35]. Hence, many people designed various methods to synthesis EDTA type chelating resin, such as grafting chloroacetate in AMPS resin. However, majority of these approaches has a rigorous synthesis condition or usually complicated in procedures. The use of polystyrene (PS) as an adsorption support is also not recent because of its outstanding physical and reactive properties [1–3,18].

This work would report the design of a novel method holding environment friendly, low-cost and efficient in order to synthesis EDTA type chelating resin as an efficient ligand for heavy metals. The PS-EDTA resin based on chloromethylated polystyrene bead with macroreticular structure was synthesized all in aqueous, and almost did not use any other toxic organic agent except materials. The chemical process has been accomplished by two steps, which forms PS-EDA resin by amination of chloromethylated polystyrene bead, and the chelating resin PS-EDTA finally synthesized by the functionalization of PS-EDA resin. The resulting PS-EDTA resin exhibits a tree type structure containing both carboxyl units and amino/imino units. The composition and structure of PS-EDA and PS-EDTA resins were characterized by using FT-IR, BET, TGA and SEM methods, meanwhile, their adsorptions for Ag (I) and other heavy-metal ions from their aqueous solutions or wastewater were also investigated by AAS method.

2. Experimental

2.1. Materials

Chloromethylated polystyrene (PSC), 1,2-ethylenediamine, chloroacetate, 1,4–dioxane, NaOH, tetrabutyl ammonium bromide (TBAB), silver nitrate, and analytical reagent grade were commercially obtained and used as received.

2.2. Preparation of PS-EDA resin

About 2 g of chloromethyl styrene-divinylbenzene copolymer was swelled in 20 mL of 1,4–dioxane in a beaker for 2 h, and then was added to a 100 mL three-necked glass flask fitted with a reflux condenser and mechanical stirrer. The alkaline solution of sodium hydroxide (2.5 g, 0.0625 mol) and the phase transfer catalyst of tetrabutyl ammonium bromide (TBAB, 0.1 g, 0.66 mmol) dissolved in 20 mL water was added in as followed. Finally, 25 mL of ethylenediamine was dropped in quickly. The reaction mixture was then heated in a water bath at 80–85 °C with continuous stirring for 6 h.

The polymer beads were filtered and rinsed thoroughly with distilled water and methanol to remove the residual impurities. The products were left to dry completely in vacuum for few days for the obtainment of PS-EDA.

2.3. Preparation of EDTA resin

About 2.52 g chloroacetate was neutralized by saturated sodium carbonate, and then added in a 100 mL three-necked glass flask fitted with a reflux condenser and mechanical stirrer. The above product, the alkaline solution of sodium hydroxide (2.5 g, 0.0625 mol) and tetrabutyl ammonium bromide (TBAB, 0.1 g, 0.66 mmol) dissolved in 20 mL water, were added in as followed. The reaction mixture was then heated in a water bath at 80–85 °C with continuous stirring for 6 h.

The resulting products were filtered and rinsed thoroughly with distilled water and methanol to remove the residual impurities. The resulting products were left to dry completely in vacuum for few days for the obtainment of final product PS-EDTA.

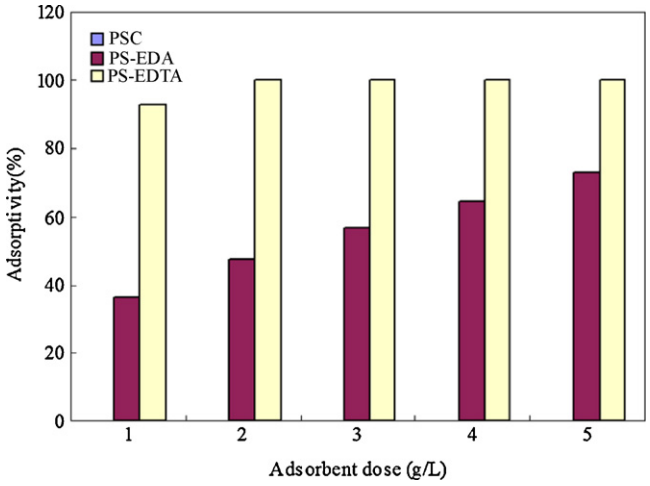

Fig. 1. Effect of adsorbent dosage on sorption of Ag (I) on PSC, PS-EDA and PS-EDTA.

2.4. Sorption of ions onto the beads

The sorption of ions onto the beads was performed in a batch experiments. For batch tests, a given amount of beads (200 mg) was added into ions aqueous solution (100 mL) at a known concentration, constant temperature of 25 °C and constant rate 150 rpm in a thermostat oscillator under dark environment. After a desired period of sorption, the solution was removed out and the concentration of metal ions was measured by AAS.

The adsorbance and adsorptivity of metal ions onto the beads were calculated according to the equations. The initial pH value of ions aqueous solution was carefully adjusted between 2.0 and 9.0 by adding a certain amount of HNO_3 or NaOH solutions with different pH values. Two linearized sorption models of Freundlich and Тёмкин isotherms were applied to analyze sorption equilibrium. The sorption kinetics of Ag (I) ions onto the beads was studied by using the pseudofirst-order and pseudosecond-order kinetic equations. Because PS-EDTA has a much higher adsorption capacity than PS-EDA, subsequent adsorption experiments with ions were performed only on PS-EDTA (show in Fig. 1).

2.5. Measurements

The FT-IR spectra of PSC, PS-EDA, PS-EDTA and PS-EDTA adsorbed Ag (I) were recorded with a Nicolet Magna-IR 550 spectrophotometer between 4000 and 450 cm^{-1} using the KBr pellet technique. The Brunauer–Emmett–Teller (BET) surface area was measured by the N_2 adsorption–desorption technique using a Micromeritics Chemisorb 2750 surface area analyzer. The thermal stability of the adsorbents was studied with a Metler Toledo Star thermogravimetric analyzer. The size and morphology of the beads were observed by a JEOC JSM-6701F scanning electron microscope (SEM) at accelerating voltages of 5 kV. A thermostat oscillators (Hai Sheng Da HQD 150L) was used for shaking all of the solutions. The concentrations of ions in solution were determined using a GBC Avanta A 5450 atomic absorption spectrophotometer (AAS). The pH of solutions was determined using a HANNA pH meter.

3. Results and discussion

3.1. Synthesis of PS-EDA and PS-EDTA

The chemical reaction of the PSC with 1,2-ethylenediamine afforded opaque, uniform and buff beads. And the finally product PS-EDTA is darker than PS-EDA. The PS-EDTA finally synthesized

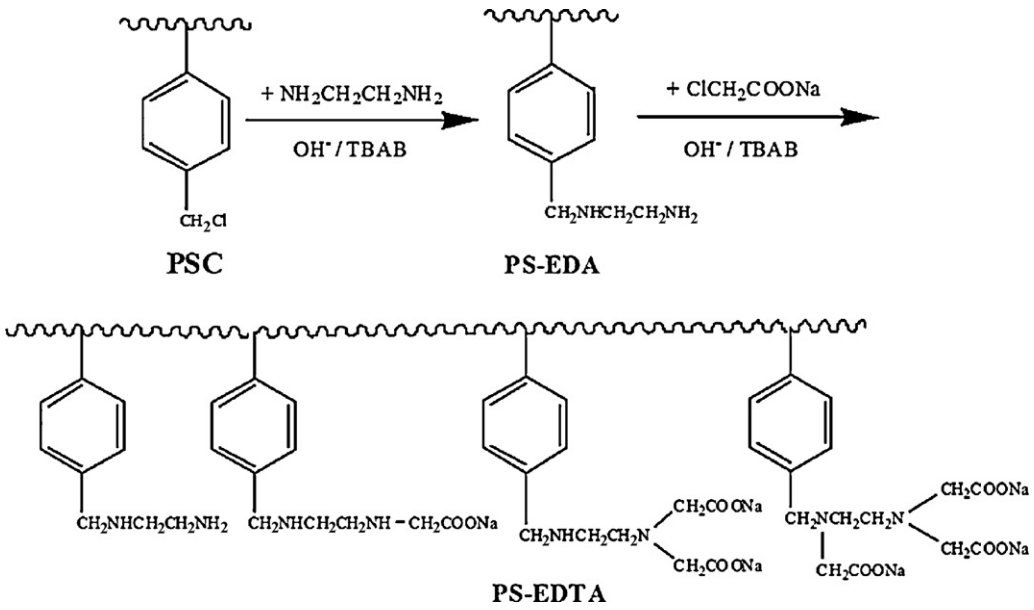

Scheme 1. Synthesis of PS-EDA and PS-EDTA.

exhibits a tree type structure containing both carboxyl units and amino/imino units with some unreacted groups (Scheme 1). The number average diameters of the products (902.1 μm, Fig. 2b) were bigger than reactant (711.7 μm, Fig. 2a), this number would increase after they adsorbed ions (Ag: 1103.9 μm, Fig. 2c; Cu: 940.6 μm, Fig. 2d).

As listed in Table 1, the reaction yields of the beads are significantly dependent on the reactant ratio, demonstrating the maximum at the PSC/EDA molar ratio of 1/25. At lower EDA content, there is even no product; consequently, abundant excess EDA was left to further reactions, resulting in much higher yield. When more EDA was added, more chlorine could be replaced and form more functions contained amino and imino, leading to the formation of more products with higher functions of carboxyl. However, too much EDA is needless. Apparently, the optimal PSC/EDA molar ratio should be 1/25 for the synthesis of PS-EDA with the maximal yield.

The alkali (NaOH or KOH) and the phase transfer catalyst (TBAB) are also necessary in the reactions.

It can be seen from Table 1 that the reaction time and temperature would hardly influence the yield of PS-EDA and PS-EDTA resin when they reached up 6 h and 80 °C, respectively.

3.2. Adsorbent characterization

3.2.1. Structure of PS-EDTA resin

To study the macro- and micro-structure of products, PS-EDA and PS-EDTA, several typical techniques such as SEM, IR, TGA, BET and elemental analysis were employed together.

The shape and surface morphologies of the beads have been studied by SEM, which are displayed in Fig. 2. It is seen from Fig. 2 that the beads all exhibit as perfect ball. The number average diameter of the PS-EDTA (902.1 μm, Fig. 2b) was bigger than PSC (711.7 μm, Fig. 2a), this number would increase after they adsorbed ions (Ag: 1103.9 μm, Fig. 2c; Cu: 940.6 μm, Fig. 2d). The surface morphology of the PS-EDTA (Fig. 2f) is different from the PSC (Fig. 2e), for which more uniform and richer aperture. It must be due to the incorporation of EDTA units into PS units and the corroded by sodium hydroxide during the reactions. These properties are favorable for producing good adsorption properties.

It is also different when it adsorbed ions (show in Fig. 2g and h), which must be due to the adsorption and adhesion of ions onto the beads.

The surface area calculated from the BET N_2 adsorption isotherm method shows that PS-EDTA (42.5 m^2/g) exhibits a higher surface

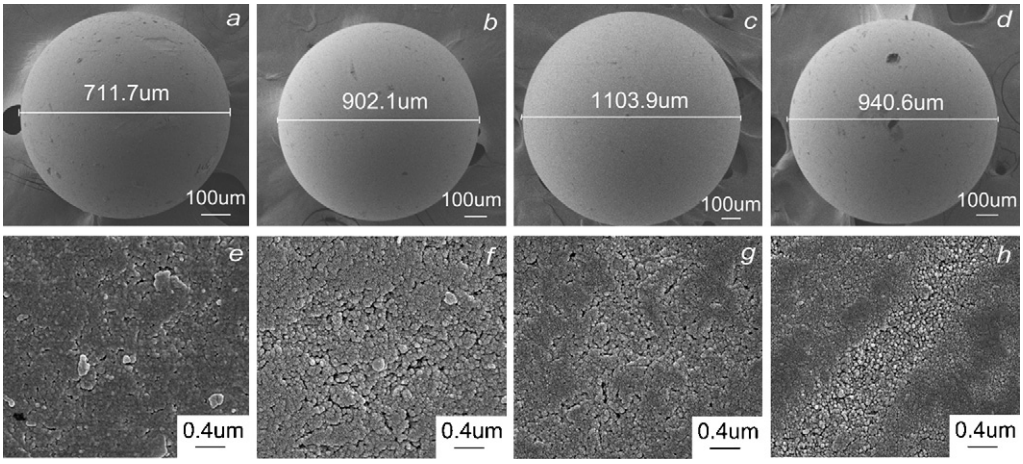

Fig. 2. SEM images of the shape and surface morphologies of the beads: (a) PSC, (b) PS-EDTA, (c) PS-EDTA after adsorbing Ag (I); (d) PS-EDTA after adsorbing Cu(II).

Table 1
Preparation of PS-EDA and PS-EDTA in aqueous.

Materials*			t (h)				T (°C)				
			2	4	6	8	r.t.	50	80	100	120
PSC:EDA	1:5	NONE	–**	–	–	–	–	–	–	–	–
		NaOH/KOH	–	–	–	–	–	–	–	–	–
		NaOH/KOH+TBAB	–	–	±	±	–	–	±	±	±
	1:15	NONE	–	–	–	–	–	–	–	–	–
		NaOH/KOH	–	–	±	±	–	–	±	±	±
		NaOH/KOH+TBAB	–	–	+	+	–	±	+	+	+
	1:25	NONE	–	–	–	–	–	–	–	–	–
		NaOH/KOH	–	–	±	±	–	±	±	±	±
		NaOH/KOH+TBAB	–	–	++	++	–	±	++	++	++

* Synthesis of PS-EDTA has a same condition except changing the main materials to PS-EDA and chloroacetate (excess).
** – No product; ± a few of product; + some product, but have low yield; ++ have a perfect yield.

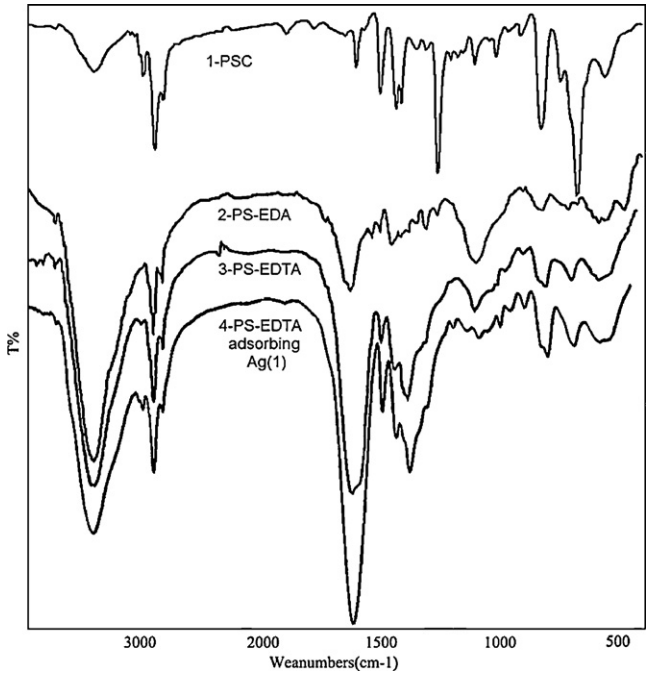

Fig. 3. IR spectra of PSC, PS-EDA, PS-EDTA and PS-EDTA after adsorbing Ag (I).

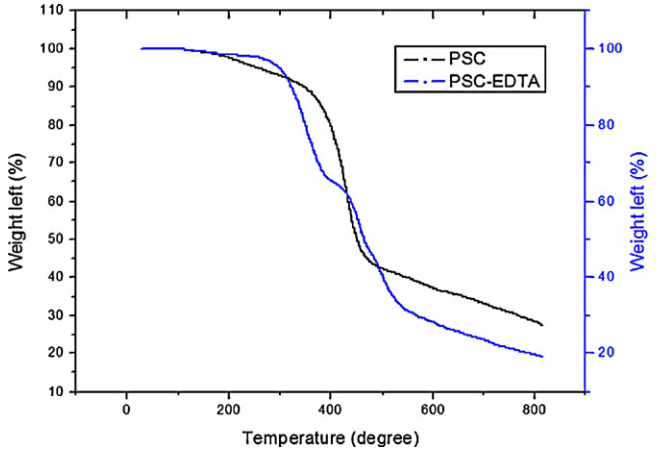

Fig. 4. The thermogravimetry (TG) curves for PSC and PS-EDTA.

area than PSC (32.0 m^2/g), possibly as a result of enhanced adsorption of N_2 in the richer micropores and aperture.

The macromolecular structure of the PS-EDTA contains different functions was studied by IR spectroscopy (Fig. 3). The broad bands at 3430 (Fig. 3, spectrum 2), 3422 (Fig. 3, spectrum 3) and 3427 (Fig. 3, spectrum 4) cm^{-1} are due to the characteristic stretching vibration of N–H bond in amino (–NH_2) and imino (–NH–) groups, respectively, strongly suggesting the presence of a large amount of amino and imino groups in the PS-EDA and PS-EDTA. The peaks at 3018 cm^{-1} (Fig. 3, spectrum 1–4) are due to the =C–H stretching vibration in benzenoid rings. The two peaks at 2919 and 2842 cm^{-1} (Fig. 3, spectrum 1), 2924 and 2853 cm^{-1} (Fig. 3, spectrum 2–4) associated with existent abundant of methylene in the polymer main chain. The peak at 1608 cm^{-1} (Fig. 3, spectrum 1) is attributed to the stretching vibration of double carbon–carbon bond in the polymer. The peak at 1634 cm^{-1} (Fig. 3, spectrum 2) is attributed to plus $v_{s\ C=C}$ and v_{amino}. The peaks at 1636 (Fig. 3, spectrum 3) and 1632 cm^{-1} (Fig. 3, spectrum 4) are associated with the stretching vibration of blue shifted carboxyl carbonyl because of connecting with polymer chain. The peak at 1593 cm^{-1} (Fig. 3, spectrum 3) is attributed to the anti-symmetric stretching vibration of amino carboxyl, which disappeared when chelating of silver ions on the resin (Fig. 3, spectrum 4). It is said that the chelation of ions in PS-EDTA happens on the amino carboxyl groups. The two sharp and strong peaks at 816 and 669 cm^{-1} might be assigned to the stretching vibration of C–Cl bond, which have disappeared in PS-EDA (Fig. 3, spectrum 2). It proves the perfect yield in synthesis of PS-EDA. The peaks around 1100 cm^{-1} are attributed to the several of amine, which changed and decreased after chelating of silver ions. It implies that the chelation also happens on the amino groups, besides carboxyl groups. The others peaks around 1400 cm^{-1} and between 600 and 800 cm^{-1} can be all attributed to benzenoid rings.

The IR spectral results suggest that the synthesis of PS-EDA and PS-EDTA in aqueous is successful and efficacious. This result is the same with the TG (Fig. 4).

The thermogravimetry (TG) curves for PSC and PS-EDTA are shown in Fig. 4. The TG curve of PSC is characterized by only one wide temperature zones: 379–472 °C. In the stage of decomposition (T = 448 °C), almost 48.32% is lost as a result of releasing the chloromethylated benzene ring and further decomposing the molecular compounds formed into large amounts of volatiles and solid char.

The TG curve of PS-EDTA shows the decomposition and weight loss to occur in three different stages. The first stage comes between 312 and 395 °C and the second stage comes from 433 °C followed by the third stage from 488 to 530 °C. In the first stage (T_1 = 338 °C), about 12.05% weight loss was observed, which might be due to the decomposition of chloroacetate that was grafted onto the PS-EDA. In the second stage of decomposition (T_2 = 460 °C), the total weight loss was about 37.99%, which might be due to decomposition of ethylenediamine that was grafted onto the PS.

In the third stage of decomposition (from 480 °C), the total weight loss was about increased from 53.88% to 19.20%, which might be due to the further decomposition of functions grafted

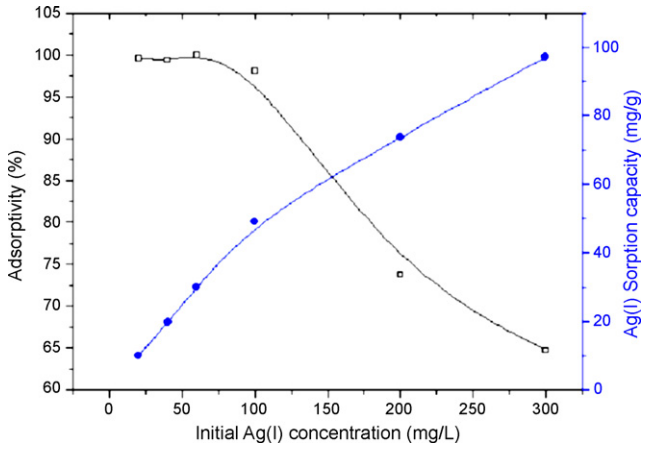

Fig. 5. Effect of initial Ag (I) concentration on sorption of Ag (I) on PS-EDTA.

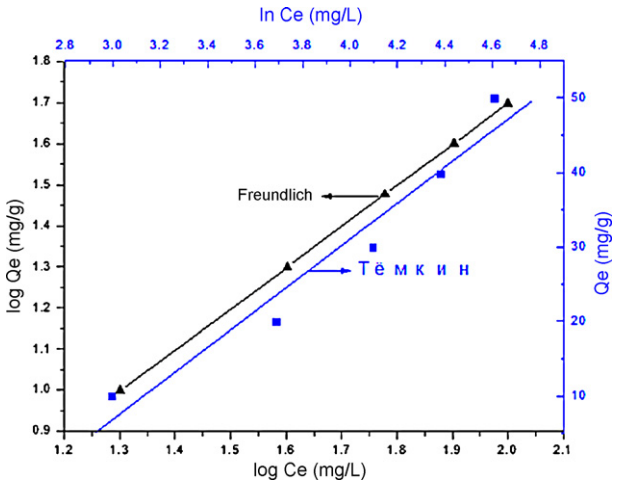

Fig. 6. Freundlich and Тёмкин plots of the sorption data in the concentration range from 20 to 100 mg/L.

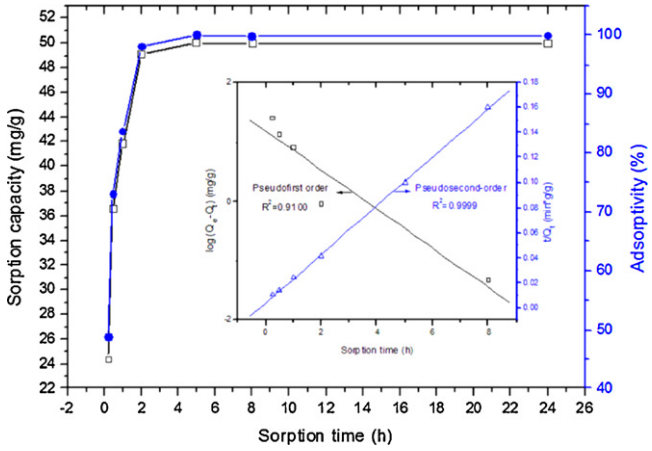

Fig. 7. Effect of sorption time on Ag (I) sorption onto PS-EDTA.

onto the polymer chains and releasing the benzene ring. Finally decomposing the molecular compounds formed into large amounts of volatiles and solid char.

The thermogravimetry of PS-EDTA results that it is stable up to 312 °C. It is said that there was no small molecule chelating agents in the PS-EDTA, in other words, the sorption of ions all happens on the polymer resin, and as such, thermal stability will not pose any problems in its practical applications.

3.3. Sorption studies

3.3.1. Sorption and its mechanism of Ag (I) onto PS-EDTA resin

To prove the occurrence of sorption and further clarify the sorption mechanism, several typical techniques such as SEM and IR, were employed together. Several sorption mechanisms were disclosed: chelation, ion exchange and so on.

To ascertain the occurrence of chelation sorption, the IR method was employed to characterize the changes of functional group before and after sorption, which are summarized in Fig. 3. The FT-IR is obviously different after adsorbing Ag (I) (Fig. 3, spectrum 4). The peak at 1593 cm^{-1} (Fig. 3, spectrum 3) disappeared, which is attributed to the anti-symmetric stretching vibration of amino carboxyl, and the peaks around 1100 cm^{-1} changed and decreased, which are attributed to the various of amine, implied that the chelation both happens on the amino groups and carboxyl groups.

3.3.2. Effect of initial Ag (I) concentration and sorption isotherm

The effect of the initial Ag (I) concentration on sorption of Ag (I) onto the PS-EDTA is shown in Fig. 5. The Ag (I) adsorbance rises significantly with an increase in Ag (I) concentration, whereas the adsorptivity declines. At a lower initial Ag (I) concentration, especially in the range of 0–100 mg/L, abundant active groups on the surface of beads can react with Ag (I) ions, resulting in a significantly increased adsorbance of Ag (I). Then the sorption process gradually becomes slow with increasing initial Ag (I) concentration. Therefore, both the Ag (I) sorption capacity and adsorptivity reach a high level at the optimal initial Ag (I) concentration of around 100 mg/L. The highest adsorptivity achieved in this study is 99.9% at the initial Ag (I) concentration of around 60 mg/L. That is to say, almost all Ag (I) ions will be adsorbed onto the resin if the initial Ag (I) concentration is lower than 60 mg/L. Two mathematical models proposed by Freundlich and Тёмкин were used to describe and analyze the sorption isotherm. The sorption data in the concentration range from 20 to 100 mg/L were selected to be modeled, considering that the sorption of Ag (I) onto the beads basically reaches equilibrium in 24 h in this concentration range. The modeled quantitative relationship between Ag (I) concentration and the sorption process is shown in Fig. 6 and the calculated correlation coefficients and standard deviations are listed in Table 2. It can be seen that the sorption isotherm behavior of Ag (I) onto the beads does not fit the Тёмкин model very well with the correlation coefficients of less than 0.99. This may result from the chemisorption processes of Ag (I) onto PS-EDTA.

3.3.3. Effect of sorption time and sorption kinetics

Sorption kinetics is studied to determine the time required to reach the equilibrium sorption of Ag (I) ions. Both Figs. 7 and 8 show representative plots of the Ag (I) sorption capacity and adsorptivity versus sorption time for the PS-EDTA resin. The Ag (I) adsorbability on the resin rises nonlinearly with increasing the sorption time. The sorption process can clearly be divided into two steps: an initial rapid step and a subsequent slow step. The sorption of Ag (I) ion onto the resin is very rapid during the initial 2 h, for which the sorption capacity and adsorptivity reach up to 49.055 mg g^{-1} and 97.41% when the initial concentration is 100 mg/L, respectively, that are 99.91% of the sorption capacity and adsorptivity for 24 h. During the sorption time from 2 to 24 h, the sorption rate becomes quite slow. The sorption capacity in the secondary long-term step contributes to a small part of the total Ag (I) sorption. The initial rapid step of Ag (I) sorption may be attributed to the physical and surface reactive sorption due to a facilely immediate interaction between Ag (I) ions and the active –NH–, $–NH_2$, –C=O and $–COO^-$ groups bared on the surface of the resin. However, the subsequent

Table 2
Isothermal model equations for Ag (I) sorption on the PS-EDTA.

Mathematical model	Equation	Correlation coefficient	Standard deviation
Freundlich	$\log Q_e = 1.0011 \log C_e - 0.3041$	0.9999	0.0008415
Тёмкин	$Q_e = 24.174 \ln C_e - 65.633$	0.9473	3.242

Table 3
Kinetic model equations for Ag (I) sorption onto the PS-EDTA.

Mathematical model	Equation	Correlation coefficient	Standard deviation	Rate constant k or initial sorption rate h
Pseudofirst-order	$\log(Q_e - Q_t) = -0.33t + 1.1903$	0.9100	0.3317	$k = 0.7599\ \text{min}^{-1}$
Pseudosecond-order	$t/Q_t = 0.0199t + 0.0029$	0.9999	0.001844	$h = 344.8\ \text{mg g}^{-1}\ \text{min}^{-1}$

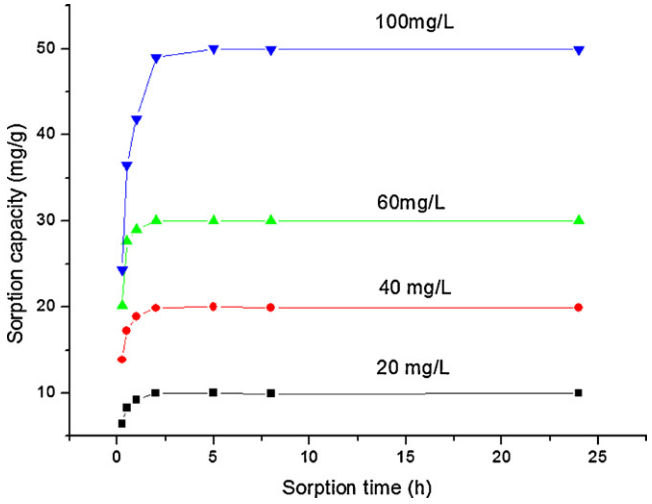

Fig. 8. The sorption capacity of Ag (I) onto PS-EDTA in $AgNO_3$ solution at different initial Ag (I) concentration.

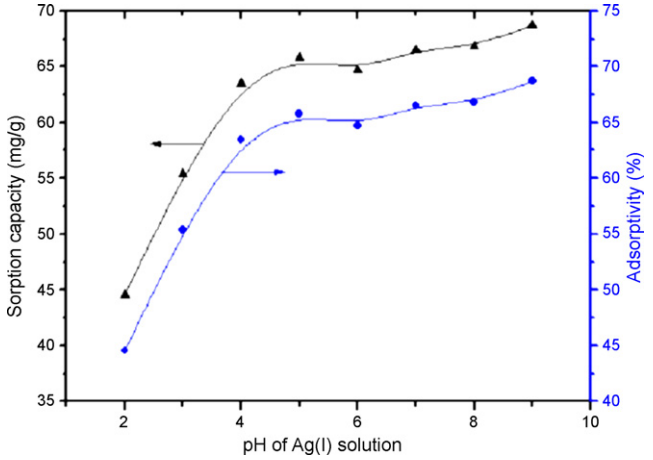

Fig. 9. Effect of solution pH on Ag (I) sorption onto the PS-EDTA.

slow step is attributable to the reactive sorption inside the beads, representing the diffusion of Ag (I) ions into the inner of the beads over a long period, besides the Ag (I) ions adhere on the surface of the beads would further hamper the diffusion of Ag (I) ions, resulting in a rather long time to reach the equilibrium sorption. It can be predicted from Figs. 7 and 8 that an even higher adsorptivity might be achieved if the sorption time were longer, indicating a great potential in the sorption of Ag (I) ions. The pseudofirst-order and pseudosecond-order kinetic equations were employed to analyze the sorption kinetics of Ag (I) ions onto the beads. The curves of $\log(Q_e - Q_t)$ versus t and t/Q_t versus t based on the experiment data are shown in Fig. 7 (inset). From the corresponding parameters summarized in Table 3, it is observed that the kinetic behavior of Ag (I) sorption onto the particles is more appropriately described by the pseudosecond-order model because of a much higher correlation coefficient and a much lower. The pseudosecond-order model was developed based on the assumption that the determining rate step may be chemisorption promoted by covalent forces through the electron exchange, or valency forces through electrons sharing between sorbent and sorbate, indicating that the sorption of Ag (I) on PS-EDTA is mainly the chemically reactive sorption. The obtained initial sorption rate of Ag (I) ions onto the beads is $344.8\ \text{mg g}^{-1}\ \text{min}^{-1}$. The loading half-time is calculated to be only 8.74 min. The kinetic data would be very useful for the fabrication and design of systems of wastewater treatment and noble metal recovery.

3.3.4. Effect of solution pH

The effect of Ag (I) solution pH 2.0–9.0 on Ag (I) sorption onto the resin has been illustrated in Fig. 9. Both the sorption capacity and the adsorptivity of Ag (I) ions increased significantly with a pH rise from 2.0 to 4.0 but increased slightly with a further pH rise from 4.0 to 9.0. This could be attributable to a competitive sorption between Ag (I) and H^+ ions due to deprotonation of amine groups and carboxyl groups on the PS-EDTA. At low pH value, the sorption of Ag (I) ions is greatly weakened because the abundant competitive H^+ ions occupy the sorption sites, whereas the protonated amine groups are deprotonated with increasing pH value, enhancing Ag (I) adsorbability. However, only a slight elevation of Ag (I) adsorbability was observed in the pH range of 4.0–9.0, suggesting that the Ag (I) adsorbability on the particles approaches saturation gradually. Therefore, the solution pH around 5.0 could be optimal for the practical application of the PS-EDTA as efficient Ag (I) sorbent.

3.3.5. Effect of adsorbent dosage

Batch experiments were conducted to determine the effect of adsorbent dosage on Ag (I) removal by PSC, PS-EDA and PS-EDTA under similar conditions (Fig. 1). The Ag (I) adsorption efficiency increased with increasing amount of adsorbents (except PSC); however, the efficiency did not increase linearly with the increase in the adsorbent dosage. The increase in adsorption with the dosage can be attributed to the increased availability of adsorption sites. Almost complete removal of Ag (I) from an initial concentration of 100 mg/L was observed at adsorbent dosages of 2 g/L for PS-EDTA. In contrast, the maximum sorption capacity of PS-EDA is 73.28%(dosage of 5 g/L), and the adsorptivity is only 47.28% at the dosage of 2 g/L. It implies that modified PS-EDTA from PS-EDA is effective and necessary. Both of the PSC sorption capacity and adsorptivity is not detected in this study.

Thus, PS-EDTA is more effective than PS-EDA. The high uptake of Ag (I) by PS-EDTA is caused by the synergy of amino and carboxyl functionality.

Table 4
Sorption of Pb(II), Zn(II) and Cu(II) ions onto PS-EDTA.

Metal ions	Initial ion concentration (mM)	Ion sorption capacity (mg/g)	Ion sorption capacity (mM/g)
Pb(II)	1.0	20.37	0.9840
Zn(II)	1.0	6.50	0.9947
Cu(II)	1.0	6.31	0.9924

3.3.6. Sorption of other ions onto the PS-EDTA resin

The adsorbability of Pb(II), Zn(II) and Cu(II) ions was also explored to investigate the sorption behavior of the PS-EDTA in this study (list in Table 4). To compare the adsorption efficiency of ions, all sorption were executed under similar sorption conditions. It is found from Table 4 that the adsorptivity is quite similar (sorption consistency = 1 mM, sorption time = 2 h, optimum pH, 25 °C).

It is reported that all of these ions can be chelated by the amino groups and/or carboxyl groups in the polymer [1]. This may be the direct cause for this result.

4. Conclusion

Synthetic yield of PS-EDA and PS-EDTA in aqueous solution by a solid-phase synthesis method exhibits the maximum at a temperature of 80 °C and indispensable both of NaOH, as alkali, and TBAB, as phase transfer catalyst. The maximum yield of PS-EDA was obtained at a PSC/EDA molar ratio of 1/25. The Ag (I) adsorbance onto the PS-EDTA resin is higher than the PS-EDA resin under similar conditions. The sorption behavior of Ag (I) onto PS-EDTA beads strongly depends on the content of amine groups and carboxyl groups. The Ag (I) adsorbability of the PS-EDTA resin can further be optimized by regulating the initial Ag (I) concentration, sorption time, and solution pH, demonstrating the highest Ag (I) adsorptivity of 99.9%. The optimal solution pH is around 5.0. The sorption process well fits the pseudosecond-order kinetics with a very rapid initial sorption rate of 344.8 mg g^{-1} min^{-1}. The sorption process mainly includes the chelation between Ag (I) and amine/carboxyl groups and the physical sorption. The PS-EDTA also demonstrates powerful divalent heavy metal ions (Pb(II), Zn(II) and Cu(II)) adsorbability.

Having a powerful adsorbability of Ag (I) and other heavy metal ions, high regeneration rate and several advantages in synthesis, good cost effectiveness, synthesis all in aqueous and moderate reaction conditions, the PS-EDTA performs a wide application prospect in the removal and even recovery of heavy-metal ions from their aqueous solutions or wastewater.

Acknowledgements

The authors gratefully acknowledge financial supports from the National Major Specific Program of Science and Technology on Controlling and Administering of Water's pollution (2008ZX07212-001-04), Key Research Program of Gansu Province (2GS064-A52-036-02, GS022-A52-082).

References

[1] X.G. Li, X.L. Ma, J. Sun, M.R. Huang, Powerful reactive sorption of silver(I) and mercury(II) onto poly(o-phenylenediamine) microparticles, Langmuir 25 (2009) 1675–1684.
[2] H. Bessbousse, T. Rhlalou, J.F. ois Verche're, L. Lebrun, Novel metal-complexing membrane containing poly(4-vinylpyridine) for removal of Hg (II) from aqueous solution, J. Phys. Chem. B 113 (2009) 8588–8598.
[3] Selva Çavuş, Gülten Gürdağ, Noncompetitive removal of heavy metal ions from aqueous solutions by poly[2-(acrylamido)-2-methyl-1-propanesulfonic acid-co-itaconic acid] hydrogel, Ind. Eng. Chem. Res. 48 (2009) 2652–2658.
[4] O. Moradi, M. Aghaie, K. Zare, M. Monajjemi, H. Aghaie, The study of adsorption characteristics Cu^{2+} and Pb^{2+} ions onto PHEMA and P(MMA-HEMA) surfaces from aqueous single solution, J. Hazard. Mater. 170 (2009) 673–679.
[5] K.M. Popat, P.S. Anand, B.D. Dasare, Selective removal of fluoride ions from water by aluminum from of the aminomethylphosphonic acid type ion exchanger, React. Polym. 23 (1994) 23–32.
[6] N. Unlu, M. Ersoz, Adsorption characteristics of heavy metal ions onto a low cost biopolymeric sorbents fromaqueous solution, J. Hazard. Mater. 136 (2006) 272–280.
[7] R. Simons, Trace element removal from ash dam waters by nanofiltration and diffusion dialysis, Desalination 89 (1993) 325–341.
[8] S.V. Joshi, S.H. Mehta, A.P. Rao, Estimation of sodium fluoride using HPLC in reverse osmosis experiments, Water Treat. 7 (1992) 207–211.
[9] X.G. Li, R. Liu, M.R. Huang, Facile synthesis and highly reactive silver-ion adsorption of novel microparticles of sulfodiphenylamine and diaminonaphthalene copolymers, Chem. Mater. 17 (2005) 5411–5419.
[10] M.R. Huang, H.J. Lu, X.G. Li, Efficient multicyclic sorption and desorption of lead ions on facilely prepared poly(m-phenylenediamine) particles with extremely strong chemoresistance, J. Colloid Interface Sci. 313 (2007) 72–79.
[11] Q.F. Lu, M.R. Huang, X.G. Li, Synthesis and heavy-metal-ion sorption of pure sulfophenylenediamine copolymer nanoparticles with intrinsic conductivity and stability, Chem. Eur. J. 13 (2007) 6009–6018.
[12] V.K. Verma, S. Tewari, J.P.N. Rai, Ion exchange during heavy metal bio-sorption from aqueous solution by dried biomass of macrophytes, Bioresour. Technol. 99 (2008) 1932–1938.
[13] M.A. Sharaf, S.A. Sayed, A.A. Younis, A.B. Farag, H.A. Arida, Removal of Hg^{2+} ions from aqueous solution by ETS-4 microporous titanosilicate-kinetic and equilibrium studies, Anal. Lett. 40 (2007) 3443.
[14] Z.R. Yue, W. Jiang, L. Wang, H. Toghiani, S.D. Gardner, C.U. Pittman, Adsorption of precious metal ions onto electrochemically oxidized carbon fibers, Carbon 37 (1999) 1607.
[15] S. Sugiyama, Y. Shimizu, T. Manabe, K. Nakagawa, K.I. Sotowa, Preparation of a hydroxyapatite film and its application in the removal and regeneration of aqueous cations, J. Colloid Interface Sci. 332 (2009) 439–443.
[16] M. Tabakci, M. Yilmaz, Sorption characteristics of Cu (II) ions onto silica gel-immobilized calix [4] arene polymer in aqueous solutions: batch and column studies, J. Hazard. Mater. 151 (2008) 331–338.
[17] E. Eroğlu, İ. Eroğlu, U. Gündüz, M. Yücel, Effect of clay pretreatment on photofermentative hydrogen production from olive mill wastewater, Bioresour. Technol. 99 (2008) 6799–6808.
[18] X. Huanga, X. Liaoa, B. Shib, Hg(II) removal from aqueous solution by bayberry tannin-immobilized collagen fiber, J. Hazard. Mater. 170 (2009) 1141–1148.
[19] D.H. Shin, Y.G. Ko, U.S. Choi, W.N. Kim, Design of high efficiency chelate fibers with an amine group to remove heavy metal ions and pH-Related FT-IR analysis, Ind. Eng. Chem. Res. 43 (2004) 2060–2066.
[20] A. Bougen, M. Rabiller-Baudry, B. Chaufer, Françoise Michel, Retention of heavy metal ions with nanofiltration inorganic membranes by grafting chelating groups, Sep. Purif. Technol. 25 (2001) 219–227.
[21] O. Genc, C. Arpa, G. Bayramoglu, M.Y. Arica, S. Bektas, Selective recovery of mercury by Procion Brown MX 5BR immobilized poly(hydroxyethylmethacrylate/chitosan) composite membranes, Hydrometallurgy 67 (2002) 53–62.
[22] H.A. Abd El-Rehim, E.A. Hegazy, A. El-Hag Ali, Selective removal of some heavy metal ions from aqueous solution using treated polyethylene-g-styrene/maleic anhydride membranes, React. Funct. Polym. 43 (2000) 105–116.
[23] L. Lebrun, F. Vallée, B. Alexandre, Q.T. Nguyen, Preparation of chelating membranes to remove metal cations from aqueous solutions, Desalination 207 (2007) 9–23.
[24] B.L. Rivas, A. Castro, Preparation and adsorption properties of resins containing amine, sulfonic acid, and carboxylic acid moieties, J. Appl. Polym. Sci. 90 (2003) 700–705.
[25] C.Y. Chen, C.L. Chiang, C.R. Chen, Removal of heavy metal ions by a chelating resin containing glycine as chelating groups, Sep. Purif. Technol. 54 (2007) 396–403.
[26] O.G. Marambio, G.D. Pizarro, M. Jeria-Orell, M. Huerta, C. Olea-Azar, W.D. Habicher, Poly (N-phenylmaleimide-co-acrylic acid)-copper (II) and poly(N-phenylmaleimide-co-acrylic acid)-cobalt(II) complexes: synthesis, characterization, and thermal behavior, J. Polym. Sci. Polym. Chem. 43 (2005) 4933–4941.
[27] B.L. Rivas, S.A. Pooley, M. Luna, K.E. Geckeler, Synthesis of water-soluble polymers containing sulfonic acid and amine moieties for the recovery of metal ions using ultrafiltration, J. Appl. Polym. Sci. 82 (2001) 22–30.
[28] H. Kas göz, New sorbent hydrogels for removal of acidic dyes and metal ions from aqueous solutions, Polym. Bull. 56 (2006) 517–528.
[29] C. Liu, B. Renbi, L. Hong, Diethylenetriamine-grafted poly(glycidyl methacrylate) adsorbent for effective copper ion adsorption, J. Colloid Interface Sci. 303 (2006) 99–108.
[30] H. Yoshitake, T. Yokoi, T. Tatsumi, Adsorption of chromate and arsenate by amino-functionalized MCM-41 and SBA-1, Chem. Mater. 14 (2002) 4603.
[31] N. Li, R. Bai, A novel amine-shielded surface cross-linking of chitosan hydrogel beads for enhanced metal adsorption performance, Ind. Eng. Chem. Res. 44 (2005) 6692–6700.
[32] T.Y. Hsien, G.L. Rorrer, Heterogeneous cross-linking of chitosan gel beads: kinetics, modeling, and influence on cadmium ion adsorption capacity, Ind. Eng. Chem. Res. 36 (1997) 3631–3638.

[33] L. Jin, R.B. Bai, Mechanisms of lead adsorption on chitosan/PVA hydrogel beads, Langmuir 18 (2002) 9765–9770.
[34] L. Dambies, C. Guimon, S. Yiacoumi, E. Guibal, Characterization of metal ion interactions with chitosan by X-ray photoelectron spectroscopy, Colloids Surf. A 177 (2001) 203.
[35] M.W.H. Evangelou, M. Ebel, A. Schaeffer, Chelate assisted phytoextraction of heavy metals from soil. Effect, mechanism, toxicity, and fate of chelating agents, Chemosphere 68 (2007) 989–1003.